Multiphase Saturation Curves of the Oxoglutarate Carrier: A Mathematical Model*

H.-G. Holzhütter

Institut für Biochemie, Humboldt-Universität
Hessische Str. 3-4 O-1040 Berlin, Germany

C. M. Sluse-Goffart and F. E. Sluse

Laboratoire de Bioénergétique
Centre Interdisciplinaire de Biochimie normale et pathologique de l'Oxygéne
Universite de Liège, Institut de Chimiie (B-6), Sart Tilman
B-400 Liège, Belgium

Abstract—Experimental data on binding and initial rate of the oxoglutarate-malate exchanger of rat-heart mitochondria exhibit a multiphase shape characterized by 3 intermediary plateaus in the saturation curve of external oxoglutarate [1]. In this paper, we present a quantitative analysis of these data on the basis of a phenomenological model which consists of a sum of Hill equations. This model leads to the assumption that there exist five iso-carriers of different sizes: one monomer exhibiting a Michaelian behaviour and four non-Michaelian oligomers. The monomer possesses a high half-saturation constant $K_1 = 14.05\,\mu M$ and the highest rate constant $k_1 = 200\,s^{-1}$, whereas the dimer exhibits the lowest half-saturation constant $K_2 = 71\,nM$, but the lowest rate constant $k_2 = 0.91\,s^{-1}$. The half-saturation constants of the other oligomers monotonously increase with their complexity. The relations observer among the amounts of the various iso-carriers suggests that the oligomers are in equilibrium with the monomer.

INTRODUCTION

The oxoglutarate carrier of rat heart mitochondria was the first antiporter carefully studied via initial rate experiments [2], as well as substrate competition experiments [3]. The results obtained so far led to the conclusion that this carrier follows a sequential mechanism involving a ternary complex of the protein and the two substrates. This catalytic complex is formed by independent rapid-equilibrium binding of substrates to the internal and external binding sites. The most striking kinetic feature of this antiporter is the "wavy" shape of the binding curves and initial rate curves [1,4–8] when varying external oxoglutarate in a wide concentration range between $50\,nM$ and $200\,\mu M$ at a fixed concentration of internal malate (counter-substrate).

In a previous paper [9], Adair's equation was applied to describe these complicated multiplateau curves. A reasonably good fit could only be achieved by taking into account exponents up to $n = 36$ indicating an extremely large protein complex. Moreover, the set of coefficients derived from binding data had to be extended by four additional terms in order to obtain a good description of the kinetic data. Although the existence of such a large-sized carrier complex

Typeset by $\mathcal{A}_{\mathcal{M}}\mathcal{S}$-TEX

cannot be excluded, an alternative hypothesis was already proposed [7,8], implying independent contributions of several oligomeric iso-carriers. A mathematical analysis based on this assumption has not been attempted so far.

The theoretical approach presented in this paper consists in the quantitative description of the experimental data by a sum of Hill equations which can be assigned to iso-carriers of different size.

DATA

The initial uptake rate of oxoglutarte (OG) was obtained via the inhibitor-stop technique calculating the slope of the linear uptake course between 0.25 s to 1 s (6–8 different incubation times) for 4 mM internal malate concentration. The binding experiments were performed with fully depleted mitochondria, since the internal-external independency and the rapid-equilibrium mechanism of the carrier were already demonstrated (for a general view cf., [7,8]). Each binding value is the mean of 5 to 10 measurements obtained with the same mitochondrial preparation. Details of the experimental procedures are given in [1,4].

MODEL

For the quantitative data analysis, we have chosen a sum of 5 Hill equations:

$$B([OG]) = \sum_{i=1}^{5} \frac{B_i}{1 + \left[\frac{K_i}{[OG]}\right]^{n_j}},$$

$$v([OG]) = \sum_{i=1}^{5} \frac{B_i}{1 + \left[\frac{K_i}{[OG]}\right]^{n_j}}. \tag{1}$$

$B([OG])$ and $v([OG])$ denote the amount of external OG bound and the rate of external OG exchanged, respectively. The parameters V_i, K_i, B_i and n_i denote the maximum rate, the half-saturation concentration, the maximum binding capacity and the Hill coefficient of the ith complex. Since the external and internal sites of the transporter are independent, only the V_i's have to be regarded as apparent parameters depending on the internal malate concentration (4 mM in our case).

The algebraic equations (1) comprise 20 unknown kinetic parameters which were estimated by nonlinear regression analysis using the program "SIMFIT" [10] on a 386-AT microcomputer. The convergency of the fitting procedure required reasonable initial guesses for the parameters which were obtained in the following manner. The parameters A_i, V_i and K_i of 4 sigmoidal contributions were estimated from the plateau levels and the middle of the ascending parts of the experimental curves. As initial estimates of the Hill coefficients, we have chosen $n = 3$ for all a contributions. The necessity to introduce a fifth contribution was derived from the observation that the plateaus of the binding curve are flatter than those of the kinetic curve indicating the existence of an overall "background" contribution in kinetics which remains invisible in the binding experiments. An estimate $n \cong 1$ for the Hill coefficient of this contribution was derived by fitting one Hill equation to the whole set of initial rate data.

RESULTS

The kinetic parameters obtained as the result of the fitting procedure are listed in Table 1 (Variant 1). From the small value of relative least square, the positive outcome of all goodness-of-fit tests available in SIMFIT [10], it can be concluded that the model provides an adequate quantitative description of the experimental data.

Table 1. Estimated kinetic parameters of the model equations (1) obtained by non-linear curve fitting.

Parameter	Unit	Fitted value (± S.D.)	
		Variant 1 (all parameters adjusted)	Variant 2 (Hill n fixed)
B_1	pmol/(mg mit. prot.)	0.95 (1.02)	1.05 (1.12)
V_1	pmol/(mg mit. prot.)·s	197.31 (0.39)	210.55 (0.39)
K_1	μM	12.32 (0.01)	14.05 (0.01)
n_1		0.98 (0.12)	1
B_2	pmol/(mg mit. prot.)	2.95 (0.12)	2.88 (0.17)
V_2	pmol/(mg mit. prot.)·s	2.52 (0.39)	2.63 (0.47)
K_2	μM	0.062 (0.02)	0.071 (0.02)
n_2		1.95 (0.22)	2
B_3	pmol/(mg mit. prot.)	8.55 (0.48)	8.44 (0.68)
V_3	pmol/(mg mit. prot.)·s	8.99 (1.33)	9.95 (1.45)
K_3	μM	0.80 (0.01)	0.781 (0.01)
n_3		3.11 (0.33)	3
B_4	pmol/(mg mit. prot.)	21.61 (0.47)	22.50 (0.57)
V_4	pmol/(mg mit. prot.)·s	58.50 (3.31)	60.11 (3.61)
K_4		5.29 (0.01)	5.31 (0.01)
n_4		4.21 (0.85)	4
B_5	pmol/(mg mit. prot.)	42.03 (1.11)	40.28 (1.28)
V_5	pmol/(mg mit. prot.)·s	123.90 (4.04)	112.41 (3.94)
K_5	μM	24.30 (0.16)	24.13 (0.06)
n_5		4.50 (0.27)	5
Sum of relative least squares (*)		0.0101	0.0105

(*) srls $\sum_{i=1}^{N} \left[\dfrac{y_i^{theor} - y_i^{exp}}{y_i^{exp}} \right]^2$

nce the Hill coefficients n are close to the set of integer values $\{1,2,3,4,5\}$, the fitting procedure repeated imposing these integer values to the Hill coefficients (Variant 2).
should be noted that with fixed integer values of exponent, the Hill equation can be considered special case of the Adair equation:

$$Y = A \frac{\sum_{i=1}^{n} i\alpha_i [S]^i}{1 + \sum_{i=1}^{n} \beta_i [S]^i},$$ (2.1)

reby the coefficients β_i and

$$\alpha_i = \begin{cases} \beta_i & \text{(binding)} \\ k_i \beta_i & \text{(kinetics)} \end{cases}$$ (2.2)

vanishing for $i \neq n$. The prefactor A in (2.1) represents the total amount of protein.
he fit obtained on the basis of Variant 2 of the model (cf., right column of Table 1 and roken lines in Figures 1 and 2) is practically of the same quality as obtained by the more eral Variant 1.
igure 3 illustrates the separate contributions of the various iso-carriers to the overall binding exchange. As can be seen from the parameters in Table 1 and from Figure 3, the Michaelian tribution ($n = 1$) exhibits a considerably higher exchange rate than the other oligomers, ereas its relative share in the overall binding of oxoglutarate can be practically neglected over whole concentration range. This accounts for the large standard deviation of the parame-B_1. The dimer possesses the largest affinity, being about two orders of magnitude higher than affinity of the monomer, whereas its rate is small but not negligible in the low concentration
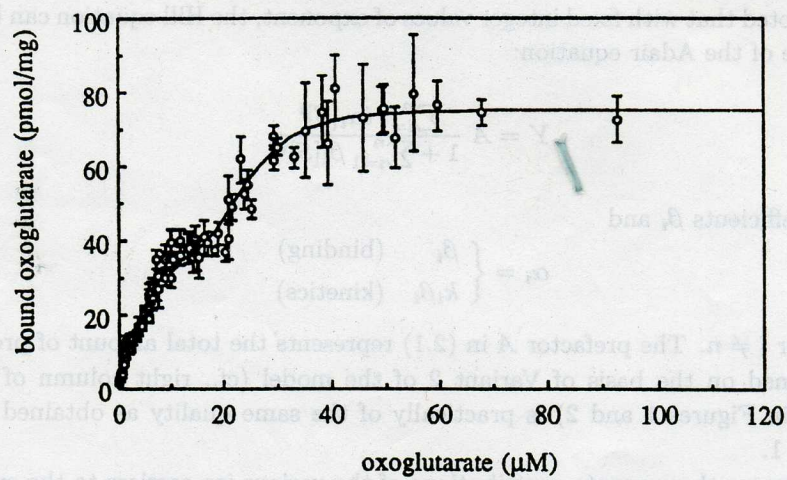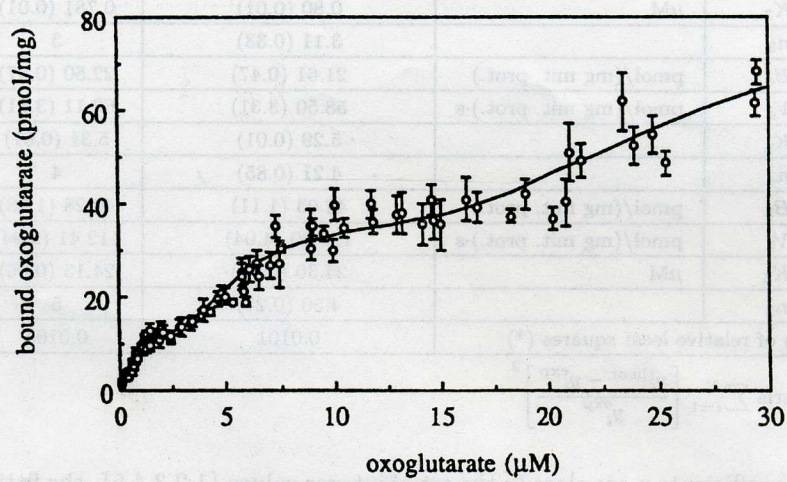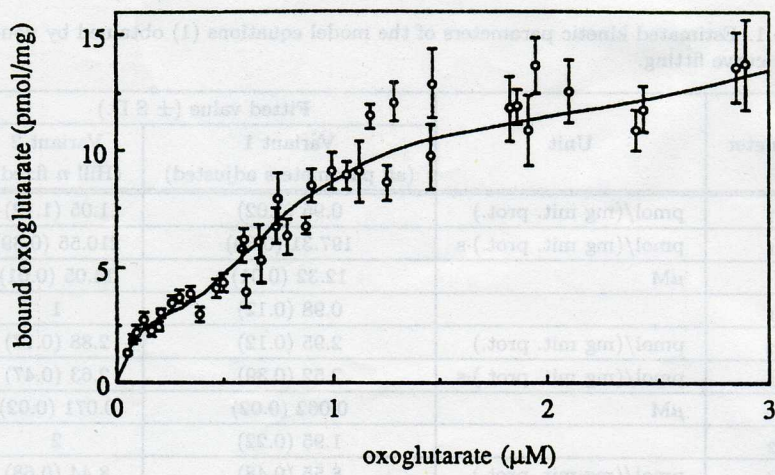
(a) 0–3 μM.

(b) 0–30 μM.

(c) 0–100 μM.

Figure 1. Carrier-bound oxoglutarate for 3 different concentration ranges of external oxoglutarate. Data are expressed in pmol/(mg mit. prot.) $\pm$ S.E.M. The unbroken line corresponds to model Variant 2.
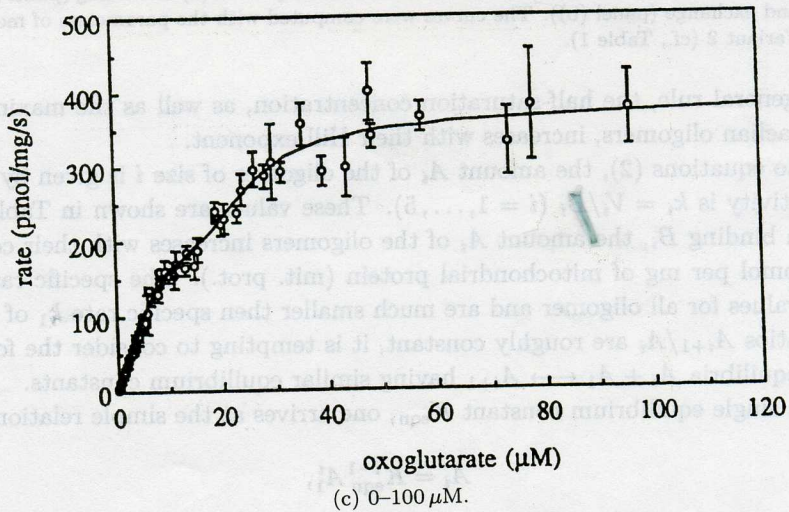
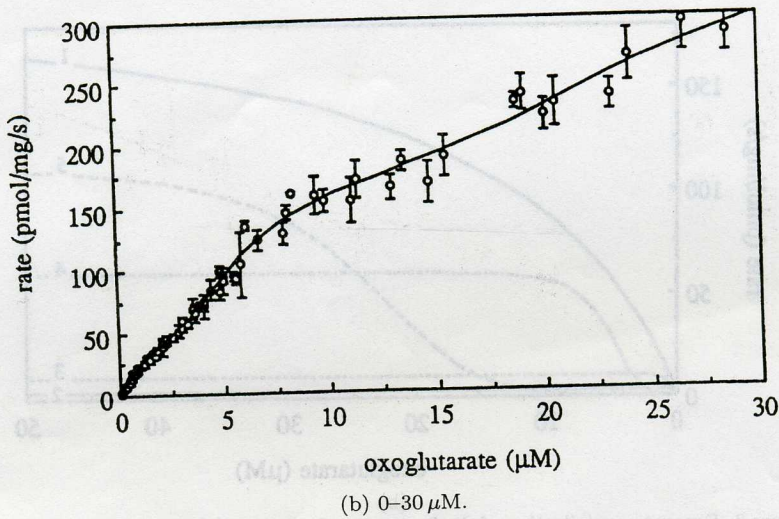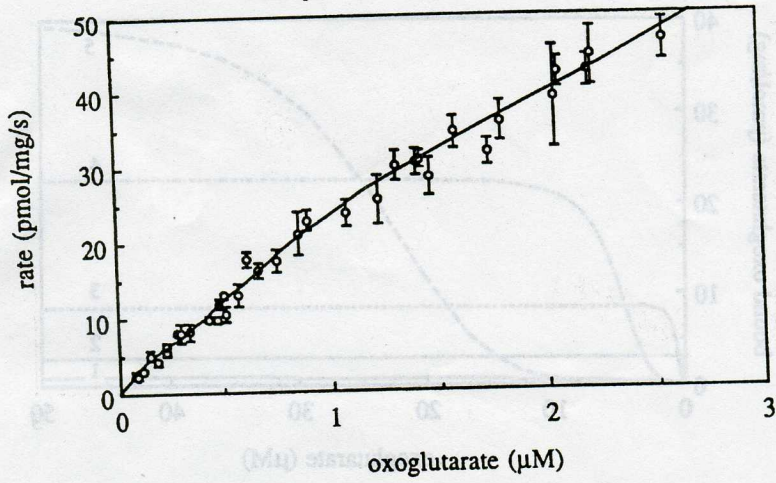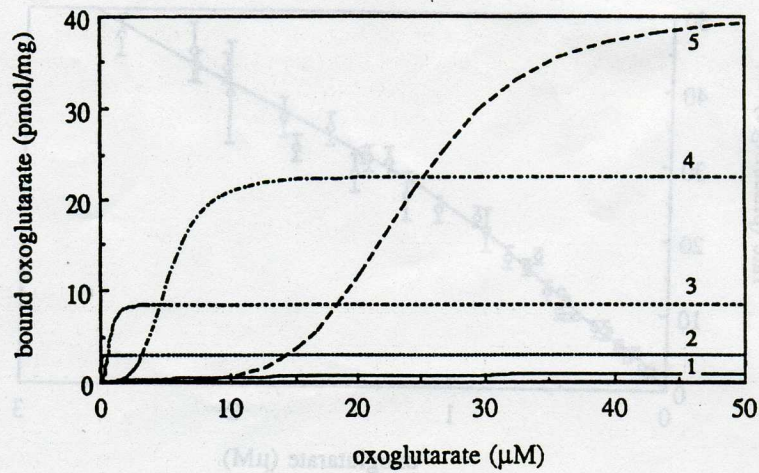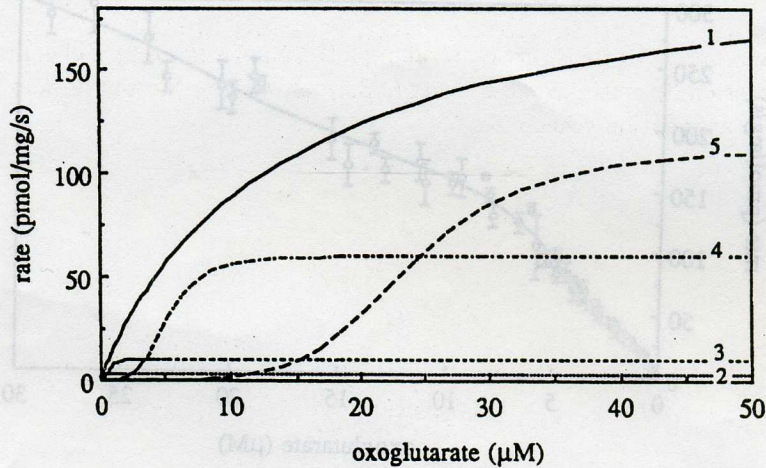(a) 0–3 μM.

(b) 0–30 μM.

(c) 0–100 μM.

Figure 2. Initial exchange rate of external oxoglutarate versus internal malate for 3 different concentration ranges of external oxoglutarate. Data are expressed in pmol/(mg mit. prot.).s ± S.E.M. The unbroken line corresponds to model Variant 2.

Figure 3. Separate contribution of the five terms of equation (1) to binding (panel (a)) and exchange (panel (b)). The curves were computed with the parameters of model Variant 2 (cf., Table 1).

range. As a general rule, the half-saturation concentration, as well as the maximum binding of the non-Michaelian oligomers, increases with their Hill exponent.

According to equations (2), the amount A_i of the oligomer of size i is given by $A_i = B_i/i$ and its specific activity is $k_i = V_i/B_i$ ($i = 1, \ldots, 5$). These values are shown in Table 2. Similar to the maximum binding B_i, the amount A_i of the oligomers increases with their complexity from 1.05 to 8.06 pmol per mg of mitochondrial protein (mit. prot.). The specific rates per sit k_i/i have similar values for all oligomer and are much smaller then specific rate k_1 of the monomer.

Since the ratios A_{i+1}/A_i are roughly constant, it is tempting to consider the formation of the oligomers as equilibria $A_i + A_1 \longleftrightarrow A_{i+1}$ having similar equilibrium constants.

Assuming a single equilibrium constant K_{eqn}, one arrives at the simple relation:

$$A_i = K_{eqn}^{i-1} A_1^i, \tag{3.1}$$

which has been tested in its linearized form

$$\ln(A_i) = i \ln(K_{eqn} A_1) - \ln(K_{eqn}). \tag{3.2}$$

Weighted lined regression leads to $K_{equ} = 1.78 \pm 0.52$ (mg mit. prot.)/pmol and $A_1 = 0.98 \pm 0.22$ pmol/(mg mit. prot.) (cf., Figure 4). It appears that the points deviate systematically
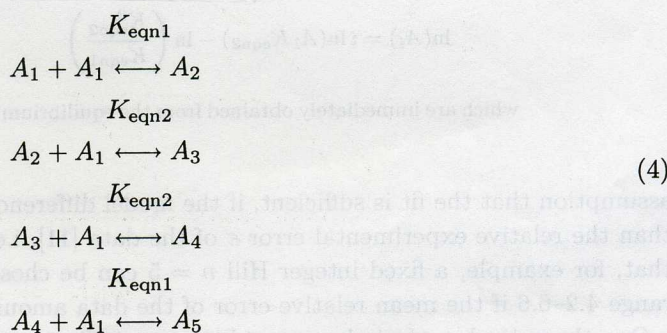
Table 2. Amount and specific rate of the oligomers. The values for the amount A_1 (second column) and for the specific rate k_i (third column) of the five oligomers were calculated according to equations (2.1) and (2.2) from the parameters of model Variant 2 listed in Table 1. The $\widehat{A}_i$-values were derived from regression analysis (Figure 5).

Complex i	Amount A_i	Specific rate (k_i)	Specific rate per site (k_i/i)	Amount $\widehat{A}_i$	
				(*)	(**)
	pmol/(mg mit. prot.)	s^{-1}	s^{-1}	pmol/(mg mit. prot.)	
1	1.05 ± 1.12	200 ± 214	200 ± 214	0.98 ± 0.22	0.98 ± 0.01
2	1.44 ± 0.09	0.91 ± 0.22	0.46 ± 0.11	$1.7. \pm 0.26$	1.43 ± 0.02
3	2.81 ± 0.23	1.18 ± 0.27	0.39 ± 0.09	2.97 ± 0.27	2.83 ± 0.02
4	5.63 ± 0.14	2.67 ± 0.23	0.67 ± 0.06	5.16 ± 0.25	5.61 ± 0.06
5	8.06 ± 0.26	2.79 ± 0.19	0.56 ± 0.04	8.98 ± 0.72	8.19 ± 0.02

(*) one single equilibrium constant

(**) two equilibrium constants (cf., legend of Figure 4)

from the unbroken line with the third point being a centre of symmetry. Therefore, we adjusted two straight regression lines to the two triplets (1,3,5) and (2,3,4) (dotted lines in Figure 4). This corresponds to an association scheme:

$$
\begin{aligned}
& \qquad\qquad K_{\text{eqn1}} \\
& A_1 + A_1 \longleftrightarrow A_2 \\
& \qquad\qquad K_{\text{eqn2}} \\
& A_2 + A_1 \longleftrightarrow A_3 \\
& \qquad\qquad K_{\text{eqn2}} \\
& A_3 + A_1 \longleftrightarrow A_4 \\
& \qquad\qquad K_{\text{eqn1}} \\
& A_4 + A_1 \longleftrightarrow A_5
\end{aligned}
\qquad (4)
$$

including two equilibrium constants. The values $K_{\text{eqn1}} = 1.49 \pm 0.09$(mg mit. prot.)/pmol and $K_{\text{eqn2}} = 2.02 \pm 0.05$(mg mit. prot.)/pmol were derived from the slopes and intercepts of the two straight regression lines (cf., legend of Figure 4). Compared with the linear regression performed with a single straight line, the standard deviations of the two equilibrium constants are considerably smaller and the predicted values for the A_i's are in better agreement with the observer values (cf., Table 2).

DISCUSSION

The modellistic approach outlined in this paper provides a good quantitative description of both binding and kinetic studies of the rat heart oxoglutarate carrier with respect to external oxoglutarate. Compared with the earlier study based on the Adair equation [9], it requires a smaller number of parameters and allows a consistent description of both binding and kinetic data with one and the same set of estimated values for the half-saturation constants and Hill exponents.

The equally good fit obtained by the two model variants (free and fixed values of the Hill n's, respectively) is obviously due to the fact that with increasing sigmoidicity of the experimental curves the range of allowed Hill n's which still yield a sufficient quantitative description of the data becomes more and more extended. This is illustrated in Figure 5, where we have simulated singmoidal "experimental" curves h_i with Hill coefficients in the interval $(0.5, 0.6, \ldots, 6.9, 7.0)$ which were then fitted by integer Hill equations $H_i(n = 1, 2, 3, 4, 5, 6)$. Under the plausible
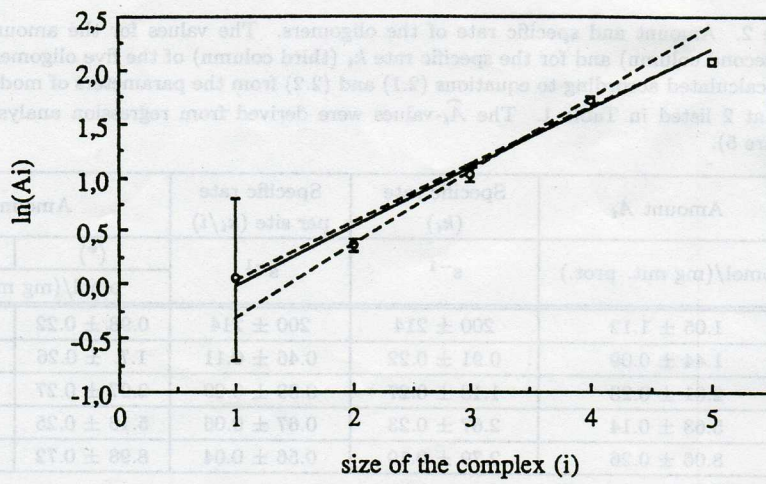
Figure 4. $\ln(A_i)$ as function of the size i of the five oligomers. The unbroken line corresponds to the linear function (3) which was adjusted to the data points by linear regression using the inverse of the standard deviations as weighting factors. The two dotted lines correspond to the linear functions:

$$\ln(A_i) = i \ln\left(A_1 \sqrt{K_{eqn1} K_{eqn2}}\right) - \ln \sqrt{K_{eqn1} K_{eqn2}} \qquad (i = 1, 3, 5)$$

$$\ln(A_i) = i \ln(A_1 K_{eqn2}) - \ln\left(\frac{K_{eqn2}^2}{K_{eqn1}}\right) \qquad (i = 2, 3, 4)$$

which are immediately obtained from the equilibrium equations of binding scheme (4).

assumption that the fit is sufficient, if the model difference $D = [(h_i - H_n)/h_i]^2$ remains smaller than the relative experimental error ε of the data [11], i.e., $D < \varepsilon$, it can be seen from Figure 5 that, for example, a fixed integer Hill $n = 5$ can be chosen for curves having a "true" n in the range 4.2–6.6 if the mean relative error of the data amounts to $\varepsilon = 0.1 (=10\%)$.

Our theoretical analysis has provided some indications that the observer complicated multiplateau shape of the rate and binding curves result from protein-protein interaction of carrier molecules within the membrane with various aggregation degrees up to 5. Limitation in the aggregation degree suggests that the largest complex form a closed structure in which the interaction sites are saturated. A recent finding that the exchange kinetics of the oxoglutarate transporter follows a simple Michaelis-Menten rate law after reconstitution into liposomes [12] might be due to the low concentration of carrier molecules in the liposome membrane so that the complexes are dissociated.

Enzyme polydispersity leading to multiplateau kinetic saturation curves of the cysteine synthetase of *Salmonella typhimurium* was analyzed, also using a sum of Hill equations as phenomenological model [13]. In the paper, the influence of modifiers on the equilibrium distribution of the various oligomers was demonstrated. In general, substrate binding should influence the protein-protein association equilibria. However, at the temperature of our experiments (2°C), it seems to be plausible that the lateral diffusion of the oxoglutarate carrier species in the membrane is slow, so that the shift of the dissociation equilibria induced by oxoglutarate binding is not detectable within the time scale of the measurements. The amounts of the different oligomers should be fixed, as implied by equation (1), to their original equilibrium values.

Finally, it has to be stated that owing to the lack of information on the quaternary structure of the carrier and its topographical arrangement within the membrane the "multicomplex self-organization hypothesis" solely derived from kinetic data remains nothing else but one possible way to look at the problem. The most severe difficulty inherent in such a view is that the independency of the internal and external carrier site(s) implies the presumed various oligomers
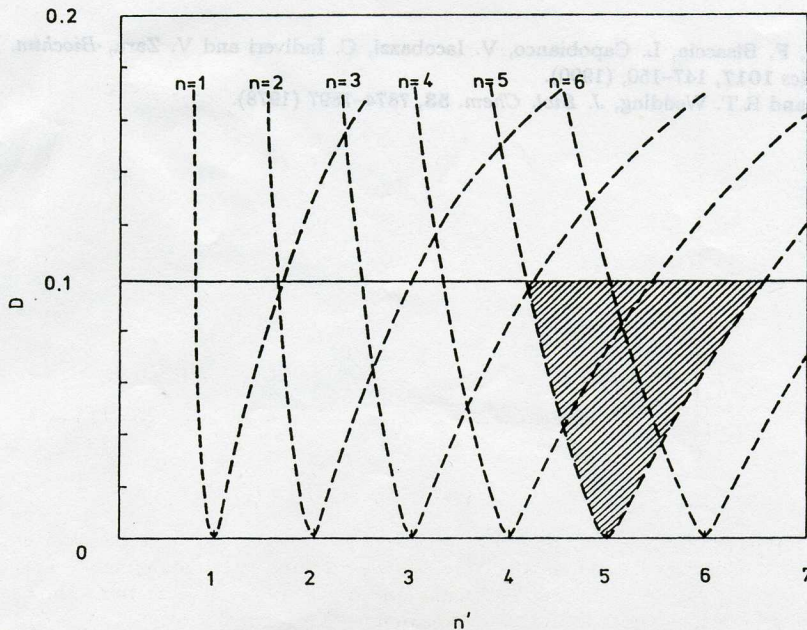
Figure 5. Distance between Hill functions having arbitrary fixed-integer exponents n, respectively. The distance:

$$D_{n,n'} = \sqrt{\frac{1}{N} \sum_{i=1}^{N} \frac{[h_i(n) - H_i(n')]^2}{h_i^2(n)}}$$

between the two Hill functions: $h_i(n) = 1/1 + (1/S_i)^n$ and $H_i(n') = 1/1 + (K/S_i)^{n'}$ was calculated whereby the exponents n' is an arbitrary (positive) real number, whereas the exponent n may assume only integer values, i.e. $n = 1, 2, \ldots$. The distance was calculated by fitting the function $H_i(n')$ at fixed value of n' (K being the only free adjustable parameter) to the data set generated by the function $h_i(n)$ at the grid $S_i = 0, 0.25, 0.5, \ldots$. As indicated by the hatched area, the distance between "true" Hill curves $h_i = 1/1 + (1/S_1)^{n'}$ and the fitting function $H_i = 1/1 + (K/S_i)^5$ remains smaller than 0.1 for $4.2 \leq n' \leq 6.6$.

display completely identical properties towards the internal substrates [5]. In other words, remains unclear how the association to higher oligomers can exclusively affect the kinetic operties with respect to the external oxoglutarate without having any influence on the internal e.

REFERENCES

1. F.S. Sluse, C. Duyckaerts, C. Liébecq and C.M. Sluse-Goffart, *Eur. J. Biochem.* **100**, 3–17 (1979).
2. F.S. Sluse, M. Ranson and C. Liébecq, *Eur. J. Biochem.* **25**, 207–217 (1972).
3. F.S. Sluse, G. Goffart and C. Liébecq, *Eur. J. Biochem.* **32**, 283–291, (1973).
4. F.S. Sluse, G.M. Sluse-Goffart, C. Duyckaerts and C. Liébecq, *Eur. J. Biochem.* **56**, 1–14 (1975).
5. G. Sluse-Goffart, F.S. Sluse, C. Duyckaerts, M. Richard, P. Hengesch and C. Liébec, *Eur. J. Biochem.* **134**, 397–406 (1983).
6. C. Duyckaerts, G. Sluse-Goffart, F.S. Sluse, X. Gosselin-Rey and C. Liébecq, *Eur. J. Biochem.* **142**, 203–208, (1984).
7. G. Sluse-Goffart and F.S. Sluse, In *Dynamics of Biochemical Systems* (Edited by A. Damjanovich, T. Keleti and L. Tron), pp. 521–535, Elsevier, Amsterdam, (1986).
8. F.S. Sluse, G. Sluse-Goffart and C. Duyckaerts, In *Anion Carriers of Mitochodrial Membranes* (Edited by A. Azzi, K.A. Nalecz, M.J. Nalecz and L. Wojtczak), pp. 183–195, Springer-Verlag, Berlin, (1989).
9. F.S. Sluse and G. Sluse-Goffart, *Abstr. Comm. 15th FEBS Meet.*, p. 114, Bruxelles, (1983).
0. H.-G. Holzhütter and A. Colosimo, *Computer Applications in Biosciences* **6**, 23–28 (1983).

12. F. Palmier, F. Bisaccia, L. Capobianco, V. Iacobazzi, C. Indiveri and V. Zara, *Biochim. Biophys. Acta Bioenergetics* **1017**, 147–150, (1990).
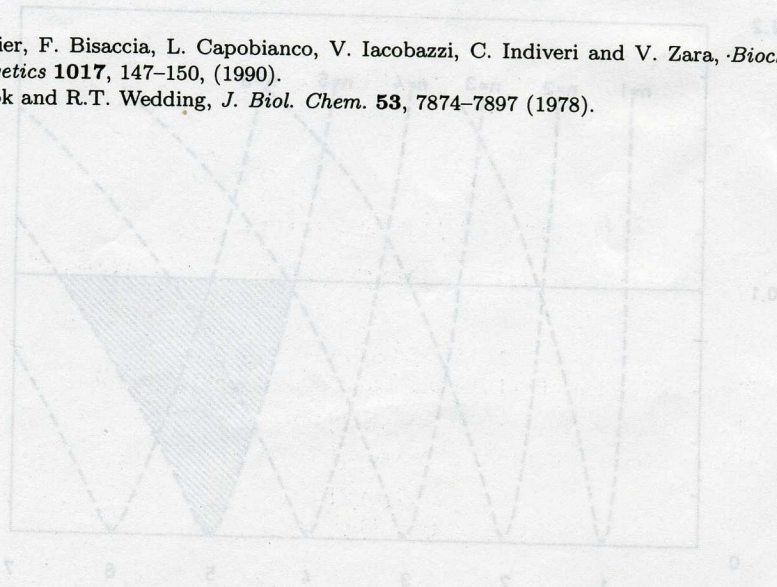13. P.E. Cook and R.T. Wedding, *J. Biol. Chem.* **53**, 7874–7897 (1978).